

Human Cortical Activity Correlates With Stereoscopic Depth Perception

BENJAMIN T. BACKUS,¹ DAVID J. FLEET,³ ANDREW J. PARKER,² AND DAVID J. HEEGER⁴

¹*Department of Psychology, University of Pennsylvania, Philadelphia, Pennsylvania 19104-6196;* ²*Department of Physiology, Oxford University, Oxford OX1 3PT, United Kingdom;* ³*Xerox Palo Alto Research Center, Palo Alto 94034;* and ⁴*Department of Psychology, Stanford University, Stanford, California 94305-2130*

Received 25 August 2000; accepted in final form 4 May 2001

Backus, Benjamin T., David J. Fleet, Andrew J. Parker, and David J. Heeger. Human cortical activity correlates with stereoscopic depth perception. *J Neurophysiol* 86: 2054–2068, 2001. Stereoscopic depth perception is based on binocular disparities. Although neurons in primary visual cortex (V1) are selective for binocular disparity, their responses do not explicitly code perceived depth. The stereoscopic pathway must therefore include additional processing beyond V1. We used functional magnetic resonance imaging (fMRI) to examine stereo processing in V1 and other areas of visual cortex. We created stereoscopic stimuli that portrayed two planes of dots in depth, placed symmetrically about the plane of fixation, or else asymmetrically with both planes either nearer or farther than fixation. The interplane disparity was varied parametrically to determine the stereoacuity threshold (the smallest detectable disparity) and the upper depth limit (largest detectable disparity). fMRI was then used to quantify cortical activity across the entire range of detectable interplane disparities. Measured cortical activity covaried with psychophysical measures of stereoscopic depth perception. Activity increased as the interplane disparity increased above the stereoacuity threshold and dropped as interplane disparity approached the upper depth limit. From the fMRI data and an assumption that V1 encodes absolute retinal disparity, we predicted that the mean response of V1 neurons should be a bimodal function of disparity. A post hoc analysis of electrophysiological recordings of single neurons in macaques revealed that, although the average firing rate was a bimodal function of disparity (as predicted), the precise shape of the function cannot fully explain the fMRI data. Although there was widespread activity within the extrastriate cortex (consistent with electrophysiological recordings of single neurons), area V3A showed remarkable sensitivity to stereoscopic stimuli, suggesting that neurons in V3A may play a special role in the stereo pathway.

INTRODUCTION

Since Wheatstone's report in 1838 that binocular disparity is sufficient to evoke a percept of depth (Wheatstone 1838), the remarkable computations that support stereopsis have been under study. Neurons selective for binocular disparity were first described in the primary visual cortex of the cat (Barlow et al. 1967; Nikara et al. 1968; Pettigrew et al. 1968). In nonhuman primates, disparity-selective cells have been identified in visual areas V1, V2, V3, V3A, V4, MT (V5), and MST (Burkhalter and Van Essen 1986; DeAngelis and Newsome 1999; Gonzalez and Perez 1998; Hinkle and Conner 2001; Maunsell and Van Essen 1983; Poggio 1995). The great ma-

jority of electrophysiological studies have been performed in V1, but disparity-selective activity in V1 is not always correlated with stereo depth perception (Cumming and Parker 1997). Although they might contribute directly as the sensory input to the vergence system, there are several respects in which the neuronal signals in V1 would need further processing to extract an unambiguous representation of stereoscopic depth (Cumming and Parker 2000; Fleet et al. 1996; Parker et al. 2000; Prince et al. 2000). For example, neurons in V1 respond to the absolute disparity of visual stimuli, showing essentially no sensitivity to relative disparity (Cumming and Parker 1999), whereas the finest stereoacuity judgments are generated psychophysically only by stimuli that contain relative disparity information (Kumar and Glaser 1992; Westheimer 1979). Absolute disparity reflects a disparity of features within the left and right retinal images with respect to anatomical landmarks on the left and right retinæ, whereas relative disparity reflects the differences in the absolute disparities of two visual features in the three-dimensional (3-D) scene. It is therefore of particular interest to investigate how the signals from disparity-selective neurons in V1 are transformed by other visual areas in extrastriate cortex (analogous to the well-characterized visual motion pathway). As a step toward that goal, we have used functional magnetic imaging (fMRI) to measure the response of several human visual areas to stimuli that contain binocular disparity.

Although human perceptual responses to binocular disparity have been studied extensively (Howard and Rogers 1995), there have been relatively few studies of how human cortical activity is related to stereo depth perception. Of these few studies, most relied on measurements of visual evoked potentials, a method that has limited spatial resolution (Braddick and Atkinson 1983; Fiorentini and Maffei 1970; Norcia and Tyler 1984; Norcia et al. 1985). A handful of positron emission tomography (PET) and fMRI experiments have been performed, focusing primarily on localizing those cortical areas that are most strongly activated by stereoscopic stimuli (Gulyas and Roland 1994; Khan et al. 1997; Nakadomari et al. 1999; Ptito et al. 1993; Rutschmann and Greenlee 1999). In contrast, we measured fMRI responses as a parametric function of disparity in each of several predefined visual cortical areas,

Address for reprint requests: B. T. Backus, Dept. of Psychology, University of Pennsylvania, 3815 Walnut St., Philadelphia, PA 19104-6196.

The costs of publication of this article were defrayed in part by the payment of page charges. The article must therefore be hereby marked "advertisement" in accordance with 18 U.S.C. Section 1734 solely to indicate this fact.

analogous to parametric measurements of contrast (Boynton et al. 1996, 1999; Wandell et al. 1999) and motion coherence (Rees et al. 2000b).

Our goals in the present study were to quantify the disparity-related responses in early cortical visual areas, and to examine how the responses of these areas are related to stereoscopic depth perception. We focused on two psychophysical measures of stereoscopic vision: the *stereoacuity threshold* and the *upper depth limit*. These measures characterize, respectively, the smallest and largest disparities that can be detected by the visual system. With fMRI, we measured cortical activity as a function of stimulus disparity. We found that responses in each of several cortical areas covaried with psychophysics and perception, and that area V3A was relatively more sensitive to binocular disparity.

METHODS

Visual stimuli

Stimuli were dynamic random-dot stereograms containing 1,000 white dots on a black background (Fig. 1). Dots were repositioned randomly at 4 Hz. Dots had a raised-cosine luminance profile 0.5° diam. The display subtended $34 \times 22^\circ$ of visual angle. The left and right eyes' stimuli were displayed side by side on a flat-panel display (NEC, multisynch LCD 2000) in a Faraday Box with a conducting glass front, positioned beyond the subjects' feet. Subjects lay on their backs and viewed the screen through approximately $\times 8$ binoculars (320 cm from the display). A pair of angled mirrors, attached to the binoculars just beyond the two objective lenses, enabled the subjects to see the two halves of the display. Vergence posture of the eyes was set, by rotating the mirrors, to be comfortable for the subject. A septum between the subject's knees prevented each eye from seeing the other's image. Subjects fixated a binocular square marker at the center of the screen, with additional (horizontal and vertical) monocular Nonius lines to allow subjective monitoring of fixation accuracy, as shown in Fig. 1 (Sheedy 1980). The fixation square was 1° wide. Dots within 2° of the center were eliminated from each half of the display.

We chose to use transparent planes, rather than corrugated surfaces or other patterns with edges in depth, on the grounds that depth edges

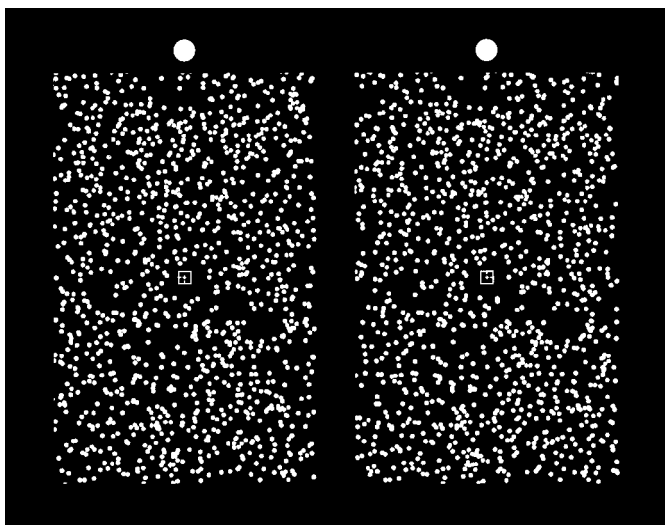


FIG. 1. Two-plane stimulus, similar to that used in the experiments. The large white dots at the top are to aid with free fusion and were not part of the actual stimulus. The fixation mark contains Nonius lines to allow subjective monitoring of fixation accuracy.

would be more likely to excite neuronal processes common to all aspects of contour identification (as were studied by Mendola et al. 1999), whereas we were interested in stereoscopic processing per se. Dots were assigned to one of two planes in depth by adding horizontal disparity to the images. Interplane disparity was varied between 0 and $\pm 4^\circ$. Perceptually, as the disparity between the planes increases, one sees first a single plane of dots (for interplane disparities less than ± 0.25 arcmin), then a thickened plane (at ± 0.25 to ± 1 arcmin), two distinct planes (± 1 arcmin to $\pm 1.5^\circ$), one plane either near or far ($\pm 1.5^\circ$ to $\pm 4^\circ$), and finally the display becomes indistinguishable from dots that are randomly placed (i.e., uncorrelated) in the two eyes' images (for disparities greater than $\pm 4^\circ$). The uncorrelated display appears to have twice the dot density of the small-disparity, correlated displays. There is no obvious rivalry in the uncorrelated displays, but the dots (being monocular) have a lustrous quality and appear to be less bright.

The left and right 2° margins of the displays contained binocularly uncorrelated dots so that both the width of the binocularly correlated images (18° of visual angle) and the width of the cyclopean images (22°) were kept constant across disparities.

Acquisition of fMRI data

The experiments were undertaken with the written consent of each subject, and in compliance with the safety guidelines for magnetic resonance (MR) research. Subjects participated in multiple MR scanning sessions on different days: one to obtain a standard, high-resolution, anatomical scan; one to functionally define the retinotopic visual areas V1, V2, V3, V3A; one to define area MT+ (in 6 of the 8 subjects); and one or more sessions to measure fMRI responses in the various experimental conditions (2 for ACH, 12 for DJH, 16 for BTB, and 1 for each of the other 5 subjects). All subjects had normal or corrected-to-normal vision. A bite bar stabilized the subjects' heads.

MR imaging was performed either on a GE 3T scanner (attention control experiment) or on a standard clinical GE 1.5 T Signa scanner (all other experiments), with custom-designed dual surface coils. Every fMRI scan consisted of 14 blocks, with 2 stimuli shown alternately (ABAB . . .). Each block lasted 18 s. The entire scan therefore lasted 252 s. Subjects were instructed to hold fixation (monitoring Nonius alignment for fixation accuracy) throughout each scan while attending spatially to the entire stimulus. In the attention control experiment, subjects performed a depth discrimination task while holding fixation (see *Experimental conditions*).

fMRI scans were performed using a T2*-sensitive, gradient recalled echo, spiral pulse sequence (Glover 1999; Glover and Lai 1998; Noll et al. 1995; Sawyer-Glover and Glover 1998). Spiral fMRI pulse sequences compare favorably with echo-planar imaging on scanners in terms of sensitivity, and spatial and temporal sampling resolution (Sawyer-Glover and Glover 1998). Pulse sequence parameters varied across experiments (Table 1) to take advantage of several hardware and software upgrades that provided improvements in the fMRI signal-to-noise ratio. Slices were either coronal or oblique (oriented perpendicular to the calcarine sulcus), with the posterior slice near the occipital pole.

Each scanning session began by acquiring a set of T1-weighted structural images using a spin echo pulse sequence (500-ms repetition time, 15-ms echo time, 90° flip angle) in the same slices as the functional images. These inplane anatomical images were aligned to the high-resolution anatomical scan of each subject's brain using custom software (Nestares and Heeger 2000), so that the functional data (across multiple scanning sessions) from a given subject were co-registered.

Experimental conditions

The full group of eight subjects was run on a subset of the stimulus conditions. Each subject in this *population average* experiment par-

TABLE 1. Pulse sequence parameters for each experiment

	Field Strength, Tesla	Repetition Time, ms	Number Interleaves	Echo Time, ms	Flip Angle, deg	Inplane Resolution, mm	Slice Thickness, mm	Number Slices
Population average	1.5	1,500	2	40	90	2.9 × 2.9	4	12
Stereoacuity and upper depth (DJH)	1.5	2,000	1	40	90	3.2 × 3.2	4	16
Stereoacuity and upper depth (BTB)	1.5	1,500	2	40	90	1.9 × 1.9	4	8
Saturation control	1.5	750	2	40	90	3 × 3	4	12
Attention control	3	750	2	30	65	2.9 × 2.9	4	12

ticipated in one scanning session that included: 1) four repeated scans of a ± 7.5 arcmin (2-plane) stimulus alternated with a zero disparity (1-plane) stimulus, and 2) five repeats of the ± 7.5 arcmin (2-plane) stimulus alternated with a blank screen. After establishing through these measurements that cortical activity depended on stereoscopic depth, we proceeded to study this dependence in greater detail in two subjects (authors BTB and DJH) in the stereoacuity and upper depth limit experiments.

In the stereoacuity experiments, two-plane stimuli were alternated with a one-plane (zero-disparity) stimulus. The interplane disparities of the two-plane stimuli were systematically varied in separate scans. The off-horopter stereoacuity experiments were similar to the stereoacuity experiments except that the stimuli were displaced in depth (relative to fixation) by some common amount. In the upper depth experiments, two-plane stimuli were alternated with a stimulus consisting of dots whose positions were uncorrelated between the left and right images. These experiments were performed on only two of the subjects because of the large number of stimulus conditions; each subject repeated each of 15 experimental conditions between 4 and 12 times in separate fMRI scans (Table 2). The repeated measurements of each stimulus condition were typically distributed across multiple scanning sessions on different days.

Psychophysical stereoacuity and upper depth limit thresholds were measured for comparison with the fMRI data. These psychophysical thresholds were measured in separate sessions using a standard forced-choice protocol. In a stereoacuity trial, 3 s of the (1-plane) zero-disparity stimulus were followed by 5 s either of the same zero-disparity stimulus or a two-plane stimulus with small (± 0.25 to ± 1.0 arcmin) disparity. In an upper depth limit trial, 3 s of the uncorrelated stimulus were followed by 5 s of either the uncorrelated stimulus or a two-plane stimulus with large (± 1 to $\pm 6^\circ$) disparity. The subject made a yes-no response to indicate whether the second interval contained stereoscopic depth. The experience was thus similar to being in the scanner, noticing that the zero-disparity (or uncorrelated) stimulus had or had not been replaced by a stimulus containing nonzero disparity. A discrimination index (d') was computed from the hit and false alarm rates (Green and Swets 1966). A value of $d' = 1$ corresponds approximately to 80% correct performance. Although these psychophysical experiments and the fMRI measurements were

TABLE 2. Number of observations (scans) for the stereoacuity and upper depth limit experiments

	DJH	BTB
Baseline	9	12 (4 for area MT+)
Stereoacuity (Fig. 5)	4, 4, 4, 4	6, 10, 9, 13
Off-horopter (Fig. 7)	4, 3, 4, 4	9, 6, 4
Upper depth (Fig. 8)	5, 4, 5, 5, 4, 5	12, 3, 5, 5, 5, 5, 6

Number of repeated measurements, in separate scans, of each stimulus condition. In general, each scan produced a simultaneous observation in all visual areas. Scan counts correspond from left to right with the abscissae of data in the indicated figures, respectively.

performed in separate sessions using different experimental apparatuses, the stimuli were as similar as possible: the two LCD monitors were calibrated to have approximately the same mean luminance and display size (see *Visual stimuli*), but the screen was viewed in the psychophysical experiments with a modified Wheatstone stereoscope (optical path length 40 cm) rather than binoculars and mirrors.

Two further experiments served as controls. In the attention control experiment, subjects performed a demanding depth discrimination task throughout each scan. Each trial lasted 6 s and consisted of a pair of 2.7-s stimulus intervals, separated by a 50-ms blank interval, and followed by a 550-ms response interval. One stimulus interval contained an interplane disparity with a base value (either ± 7.5 or 0 arcmin), and the other interval contained an increment over and above the base value. The subject indicated which interval had greater depth by a button press. Throughout each fMRI scan, subjects performed three successive trials of the depth discrimination task at a base disparity of ± 7.5 arcmin, followed by three trials of the task at a base disparity of 0 arcmin, and so on. Subjects practiced the task extensively before scanning until their thresholds reached asymptotic performance. Feedback was not provided to subjects during the fMRI scans. Task difficulty was controlled by a 2-down 1-up staircase procedure (i.e., the disparity increment varied slightly from trial to trial) to keep the stimuli at the subjects' psychophysical threshold. The stimuli in this experiment were limited to the peripheral visual field ($>4^\circ$) to minimize the possibility that subjects might rely on differential shifts of spatial attention to perform the task at the two different base disparities, e.g., to avoid the possibility of attending centrally for 0 arcmin and peripherally for ± 7.5 arcmin. The attention control experiment was performed in one scanning session, for each of two subjects (BTB and DJH). During that scanning session, each subject participated in 1) four repeated scans of depth discrimination alternating between large (± 7.5 to ± 9.0 arcmin) and small (0 to ± 2 arcmin) interplane disparities, 2) four repeated scans of essentially the same stimulus conditions, but without performing the depth discrimination task and without the threshold changes in interplane disparity (to prevent subjects from covertly performing the task), and 3) four repeated scans of the ± 7.5 -arcmin stimulus alternated with a blank screen.

The response saturation control experiment was similar to the two-plane/one-plane (± 7.5 vs. 0 arcmin interplane disparity) condition of the population average experiment, except that stimulus contrast was lower. Light gray dots were shown against a medium gray background (15% Michelson contrast). The response saturation experiment was performed in one scanning session, for each of three subjects (BTB, DJH, and ACH). During that scanning session, each subject participated in 1) four repeats of the low-contrast, ± 7.5 arcmin (2-plane) stimulus alternated with the low-contrast, zero disparity (1-plane) stimulus, and 2) four repeats of the low-contrast, ± 7.5 arcmin (2-plane) stimulus alternated with a blank (gray) screen.

Analysis of fMRI data

Details of the analysis methods have been described previously (Heeger et al. 1999). Data from the first 36-s cycle were discarded to avoid effects of magnetic saturation and to allow the hemodynamics to reach steady state (noting that the full duration of the hemodynamic

impulse response is well over 20 s). Data from each scan were analyzed separately in each of the identifiable visual areas (see *Localization of visual areas*). We computed the fMRI response amplitudes and phases by 1) correcting for any residual head movements during each scan using custom software (Nestares and Heeger 2000); 2) removing the linear trend in the time-series to compensate for the fact that the fMRI signal tends to drift very slowly over time (Smith et al. 1999); 3) dividing each voxel's time series by its mean intensity (to convert the data from arbitrary intensity units to units of percent signal modulation, and because the mean image intensity varies substantially with distance from the surface coil); 4) averaging the resulting time series over the set of voxels corresponding to the stimulus representation within a visual area; 5) calculating the amplitude and phase of the best fitting 36-s period sinusoid (the phase is a measure of the temporal delay of the hemodynamic response relative to the onset of the stimulus cycle and the amplitude is a measure of the level of modulation of cortical activity); and then 6) extracting the projected amplitude (as described in Heeger et al. 1999). Finally, we computed the mean and standard error of the mean (SE) of the amplitudes across repeated scans of each stimulus condition. The final mean amplitude represents our estimate of the response of a given visual area for a given stimulus condition.

In addition, correlation maps were computed by calculating a correlation coefficient between the best-fitting 36-s period sinusoid and the corresponding time series, separately for each voxel (Fig. 3). The correlation is a measure of signal-to-noise (Engel et al. 1997); it takes on a value near 1 when the signal modulation (the 36-s period component of the fMRI time series) is large relative to the noise (the other frequency components of the time series), and it takes on a value near 0 either when there is no signal modulation or when the signal is overwhelmed by noise. The correlation maps thus locate regions that responded reliably to the periodic changes in the stimuli. Amplitude and correlation differ in that measurement noise (both noise inherent in the MR signal and physiological noise) directly reduces correlation, but affects only the variance and not the true mean of the response amplitude measurements.

Localization of visual areas

Following well-established methods (DeYoe et al. 1996; Engel et al. 1994, 1997; Sereno et al. 1995) the polar angle component of the retinotopic map was measured by recording fMRI responses as a stimulus rotated slowly (like the second hand of a clock) in the visual field. To visualize these retinotopy measurements, a high-resolution MRI of each subject's brain was computationally flattened (Teo et al. 1997; Wandell et al. 2000). In each hemisphere, areas V1, V2d, V2v, V3d, V3v (also known as VP), and V3A were identified. Area boundaries were drawn by hand on the flat maps near reversals of polar angle, leaving a gap of approximately 2 mm near the reversals that was unassigned to either area. We found neither ventral/dorsal nor left-/right-hemisphere differences in activity within a given cortical

area. Hence, areas V2d and V2v from both hemispheres were combined for analysis into a single region designated V2, areas V3d and V3v were combined into V3, V1 was combined across the two hemispheres, and V3A was combined across the two hemispheres. Figure 2 shows the locations of some of the areas in the right hemisphere of *subject BTB*'s brain. V3A can be seen at the fundus of the transverse occipital sulcus, in agreement with previous reports (Tootell et al. 1997). Our retinotopy measurements were too noisy to map areas V4v, V7, and V8 with complete confidence in all subjects.

For some of the experiments, the data were also analyzed in area MT+ (also known as V5), an area of the human brain that is believed to be homologous to monkey areas MT and MST. However, data collected from *subject BTB* using the eight-slice protocol (Table 1) could not be analyzed in MT+ because the slices did not cover this area. Following previous studies (Tootell et al. 1995; Watson et al. 1993; Zeki et al. 1991), area MT+ was identified based on fMRI responses to stimuli that alternated in time between moving and stationary dot patterns. The dots (small white dots on a black background) moved (10°/s) radially inward and outward for 18 s, alternating direction once every second. Then the dot pattern was stationary for the next 18 s. This moving/stationary cycle was repeated seven times. We computed the cross-correlation between each fMRI voxel's time series and a sinusoid with the same (36 s) temporal period. We then drew MT+ regions by hand around contiguous areas of strong activation, lateral and anterior to the retinotopically organized visual areas. MT+ was identified in this way for six of the eight subjects.

The procedures to define the visual areas were performed only once per subject. Because the fMRI data recorded during successive scanning sessions in a given subject were co-registered (see above), we could localize these areas from one scanning session to another.

Reference scans

We defined a subregion of each visual area based on responses to a reference stimulus. The reference scan responses were used to exclude unresponsive voxels, e.g., brain regions that would have responded to visual field locations outside the $34 \times 22^\circ$ stimulus aperture, and voxels that had too little overlap with gray matter. The reference scans (for all but the attention control experiment) consisted of a two-plane stimulus with an interplane disparity of ± 7.5 arcmin shown in alternation with a blank screen. One reference scan was run during each scanning session, typically as the first scan in the session. Voxels that were unresponsive in the reference scans were discarded in the analysis of all subsequent scans in that scanning session. Responsive voxels were defined as those for which the fMRI time series was well correlated ($r > 0.4$ and, consistent with hemodynamics, a 0- to 9-s time lag) with a sinusoid of period 36 s. For the attention control experiment, the reference scan stimuli alternated between two planes (± 7.5 arcmin) and one plane (zero disparity), instead of alternating with a blank screen. This was done because the goal of this experiment was to determine whether the areas that were

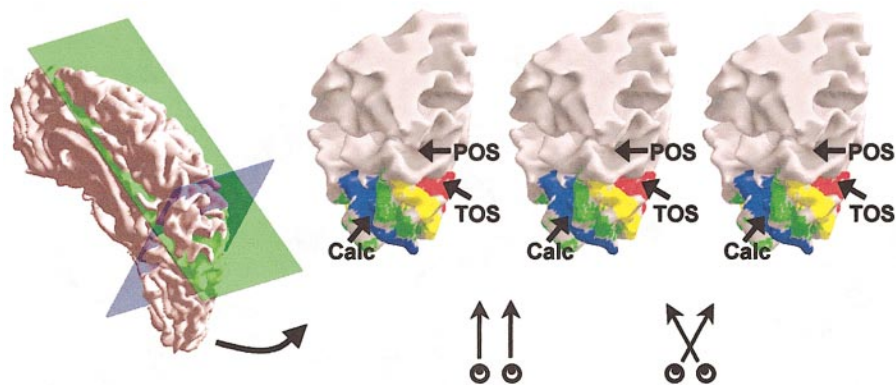


FIG. 2. Retinotopic visual areas. The stereogram shows the locations of dorsal visual areas in the right occipital lobe of *subject BTB*, viewed from above. Visual areas: V1 (blue), V2d (green), V3d (yellow), and V3A (red). Landmarks are as follows: Calc, calcarine sulcus; POS, parietal-occipital sulcus; TOS, transverse occipital sulcus. All but 1 mm of gray matter have been removed to better reveal the brain structure.

activated during passive viewing would again be activated when subjects performed the depth discrimination task.

Our results were not biased by subselecting voxels based on the reference scan responses. The reference scans activated large, contiguous regions of visual cortex, corresponding to the retinotopic representations of the stimuli within each visual area (Fig. 3, *B* and *C*). The particular interplane disparity used in the reference scans (± 7.5 arcmin) was chosen because it gave stronger responses than did a single plane, in all of the studied visual areas. The correlation threshold was chosen to exclude only gray matter voxels that corresponded retinotopically to visual field locations outside the $34 \times 22^\circ$ stimulus aperture, and the results were similar when the data were reanalyzed for a range of different correlation thresholds from $r > 0.2$ to $r > 0.5$. There is evidence for spatial clustering of disparity-tuned neurons in macaque cortical visual areas V2 (Hubel and Livingstone 1987; Hubel and Wiesel 1970; Peterhans and von der Heydt 1993; Roe and Ts'o 1995) and MT (DeAngelis and Newsome 1999). Organization of this type is presumably invisible in our fMRI measurements because it

occurs on a spatial scale (~ 1 mm) that is much smaller than the size of our voxels ($\sim 3 \times 3 \times 4$ mm).

A second use of the reference scans was to validate comparisons of data collected with the different scanning protocols (Table 1). This comparison was performed for *subject BTB* because we measured reference scan responses for that subject using each of the protocols. The reference scan responses in all of the visual areas were highly reproducible; the 68% confidence interval obtained from one protocol contained the respective means from each of the other protocols.

Normalized responses

We normalized the responses of each visual area and each stimulus condition by dividing by the mean responses to a baseline stimulus condition in each visual area. The normalized responses are analogous to selectivity indices (e.g., disparity- or direction-selectivity indexes) that are commonly reported in single-unit electrophysiology studies. The normalized responses characterize how responsive a cortical area

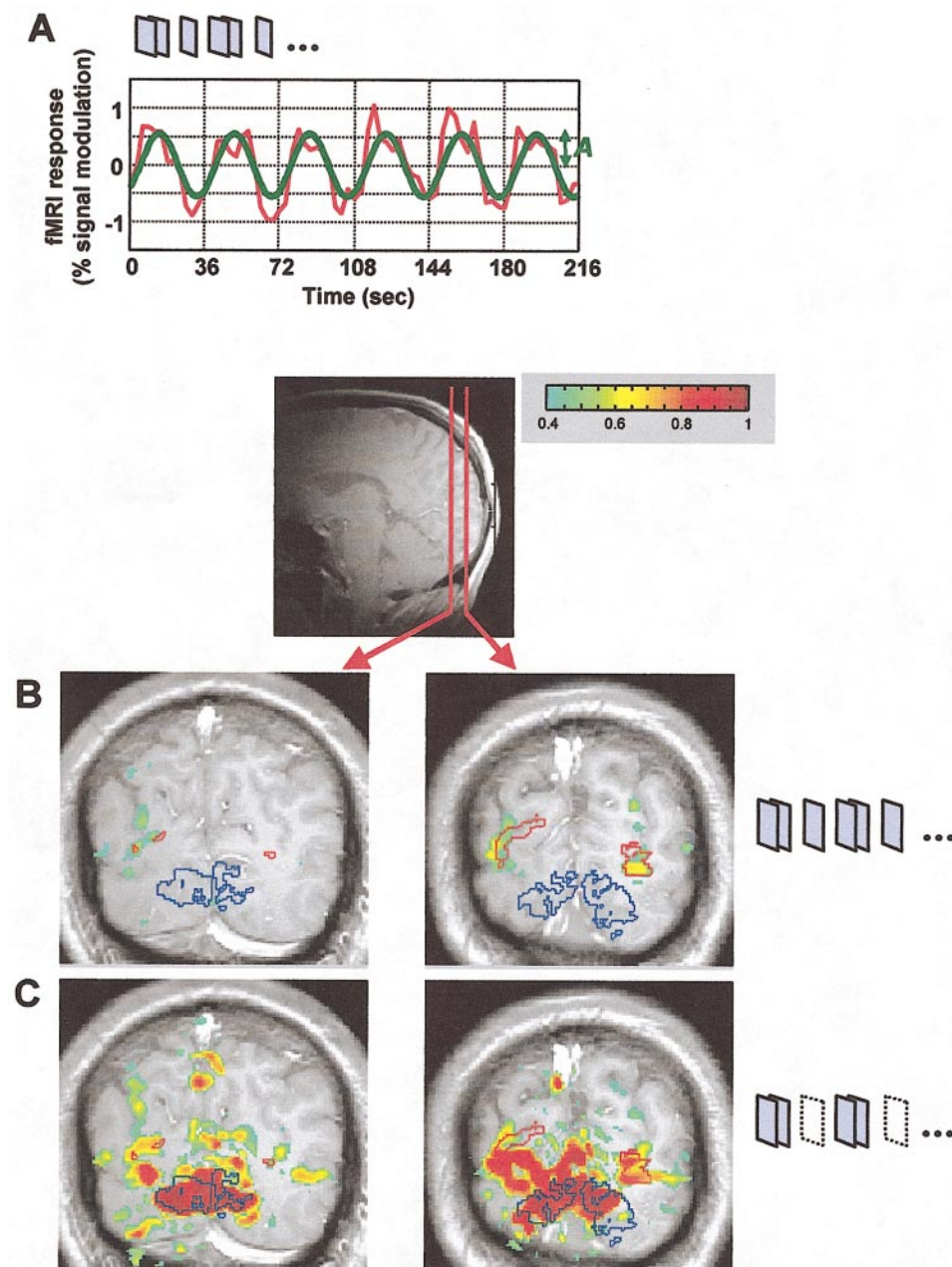


FIG. 3. Example of functional magnetic imaging (fMRI) responses from a single subject. *A*: fMRI time series (red curve), averaged across 4 repeats of the 2-plane/1-plane scan, and averaged across the gray matter voxels corresponding to the stimulus representation within V3A. Green curve, best fitting sinusoid. Amplitude (*A*) of best fitting sinusoid reflects the modulation in cortical activity evoked by the stimulus alternations. *B*: correlation maps averaged from 4 repeats of the 2-plane/1-plane scan. Slice position and orientation indicated in the sagittal section. Gray scale, anatomical slice from the subject's brain. Colored pixels, fMRI time series correlated strongly with the 2-plane/1-plane stimulus alternations ($r > 0.4$, 0- to 9-s time lag). Red contour, subregion of area V3A in these slices. Blue contour, subregion of V1 in these slices. *C*: correlation maps (same slices and format as *B*) averaged from 4 repeats of the 2-plane/blank scan.

is to the change between two visual stimuli, relative to its response to a baseline stimulus condition. The normalized responses are thus complementary to the unnormalized responses, being particularly useful when comparing responses across subjects, cortical areas, and stimulus conditions.

The baseline responses were measured using stimulus conditions identical to those used for the reference scans (± 7.5 arcmin alternated with a blank screen). The baseline responses were averaged over a set of repeated scans (between 4 and 9), that excluded those scans used to select the subregions of each visual area (see *Reference scans*). The three panels of Fig. 4 plot the unnormalized responses, the baseline responses, and the normalized responses. Figures 5–10 plot responses that have also been normalized in this way. The normalized responses are expressed in units of percent, that is the percentage of the baseline response evoked by each stimulus condition. For example, a normalized response of 50% in the stereoacuity experiment would mean that alternating the two-plane stimulus with the one-plane stimulus evoked one-half the modulation in cortical activity as alternating the two-plane stimulus with a blank screen. Normalizing the responses in this way simplified the interpretation of the results because it compensated for any differences in the hemodynamic response across individuals and/or across cortical areas within an individual. One visual area might have been more responsive to all stimulus conditions than another visual area for reasons unrelated to the stimulus disparity. First, the stimuli might have been more effective in driving one visual area than another (e.g., in terms of spatial or temporal frequency content). Second, the vasculature, and consequently the hemodynamic response, might have differed between the visual areas and/or between subjects (Aguirre et al. 1998). Third, errors in identifying the visual areas (for example, by including different fractions of unresponsive tissue, such as white matter or cerebrospinal fluid) could have introduced a systematic scaling of the measured responses in one of the areas. Fourth, some areas may have been more susceptible to the influences of attention. To the extent that such effects were multiplicative and of the same size for all stimulus conditions, they were mitigated by normalization.

Statistics

One-tailed *t*-tests were used to determine the statistical significance of the responses by testing the null hypothesis that the mean response amplitudes were zero, i.e., that there was no modulation of cortical activity. Analogous *t*-tests were used to compare the relative responses across visual areas, e.g., to show that the responses in area V3A were larger than those in other visual areas. These statistical tests were always performed on the unnormalized responses. These were typically more conservative tests than the comparable tests on the normalized responses.

The error bars for the normalized responses in Figs. 4–10 were computed using a parametric bootstrapping procedure (Efron and Tibshirani 1993). This procedure works by randomly resampling from the measured responses. In particular, we randomly sampled values from the normal distributions defined by the mean and SE for each test condition and for the baseline (reference scan) condition. The number of samples was equal to the actual number of repeated measurements for each condition. We then analyzed the resampled data as described above. These steps were repeated 1,000 times for each condition in each visual area. Finally, 68% confidence intervals were computed from the resulting bootstrapped response distributions.

Error bars estimate different quantities in different Figs. In Fig. 4, bars show confidence for the population mean (based on 8 subjects, 6 for area MT+). In Figs. 5–8 bars show confidence for the mean of a single subject in a given condition. In Figs. 9 and 10 bars show confidence for the mean of the two (and 3) particular subjects, estimated as the square root of the summed variance for subject means, divided by number of subjects.

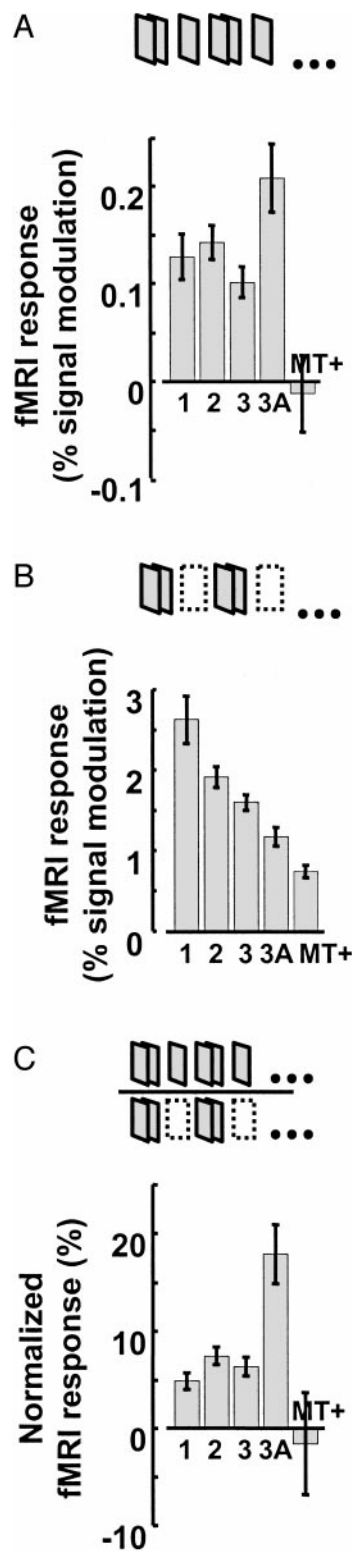


FIG. 4. Activity in early visual cortex was larger for stimuli with stereoscopic depth than for a single flat plane. *A*: fMRI responses in each of several visual areas, averaged across 8 subjects, during scans that alternated between 2 planes (± 7.5 arcmin disparity) and a single plane (zero disparity). *B*: baseline responses to alternation between the 2-plane stimulus and a blank screen. *C*: normalized responses computed by dividing the responses in *A* by those in *B*. The responses were normalized separately for each subject, before averaging across subjects, to compensate for the inter-subject differences. Error bars represent 1 SE across subjects (i.e., to yield a confidence interval on the population mean).

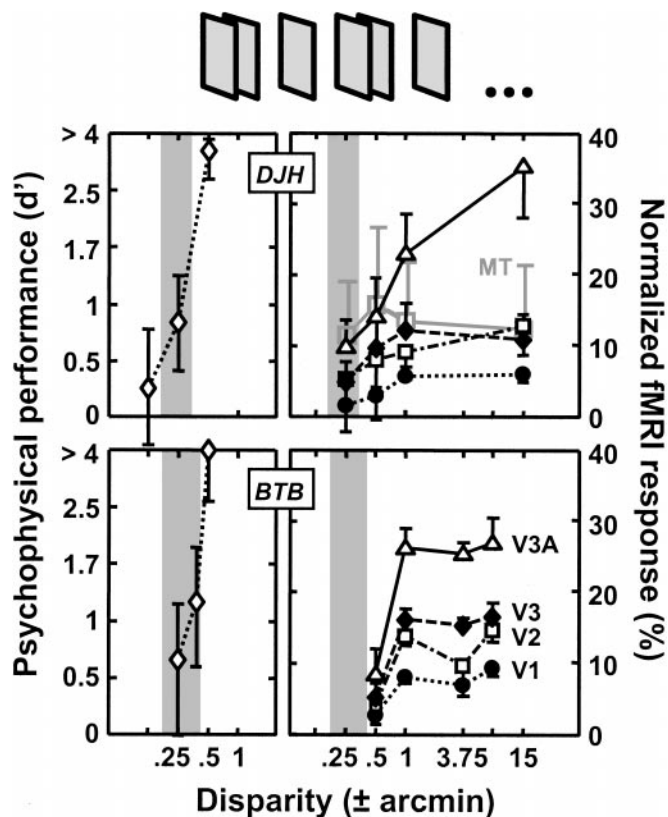


FIG. 5. Cortical activity and psychophysical performance in the stereoacuity experiment. *Left panels:* psychophysical performance for discriminating 2-plane stimuli from a single (zero-disparity) plane. Discrimination index (d') is plotted as a function of interplane disparity. Error bars represent 95% confidence intervals. The shaded region corresponds to the range of interplane disparities near threshold, i.e., where the extrapolated 95% confidence interval includes $d' = 1$. *Right panels:* normalized fMRI responses in 4 visual areas (labeled in the figure). Error bars represent 68% confidence intervals computed from the bootstrapped response distributions (see METHODS). The shaded region has been copied from the panels on the left.

Eye tracking

Eye-tracking measurements were performed to determine whether patterns of eye movements might account for some of our results. These experiments were performed in a psychophysical laboratory, not in the MR scanner, but the stimuli were identical to those displayed in the scanner, calibrated for the same luminance, contrast, and display size. Although it would have been ideal to record eye movements and acquire functional data simultaneously, that was not possible with the equipment we had available. We recorded eye movements using an infrared eye-tracking system (Ober 2, Timra, Sweden) that sampled horizontal and vertical eye positions at 100 Hz.

RESULTS

Population average

Activity in early visual cortex was larger for stimuli with stereoscopic depth than for a single flat plane. A representative example from one subject is shown in Fig. 3. Figure 3A plots the fMRI time series (red curve) averaged across the set of gray matter voxels corresponding to the stimulus representation within V3A, for scans that alternated between two planes (± 7.5 arcmin) and a single plane (zero disparity). Note that the signal increased during the presentation of the two-plane stimulus and decreased during the presentation of the one-plane

stimulus. The thick green curve is the best-fitting sinusoid. The amplitude of this sinusoid reflects the difference in cortical activity evoked by the two stimuli.

Figure 3, *B* and *C*, shows examples of correlation maps (see METHODS) superimposed on the inplane anatomical slices from one subject's brain. The correlation between the fMRI time series and the best-fit sinusoid at each voxel is a measure of the signal-to-noise ratio (Engel et al. 1997); it takes on a value near 1 when the stimulus-driven signal modulation is large relative to the noise in the fMRI time series, and it takes on a value near 0 either when there is no signal modulation or when the signal is overwhelmed by noise. Figure 3*B* shows regions, including V3A (indicated by the red contour), where the cortical activity modulated strongly with the two-plane/one-plane stimulus alternations. Figure 3*C* shows regions, including V1 (indicated by the blue contour), where the cortical activity modulated strongly for stimuli that alternated between two planes (± 7.5 arcmin) and a blank screen.

We observed additional regions of visual cortex that also gave large responses in the two-plane/one-plane scans (Fig. 3*B*), including a ventral area, perhaps V4v or V8 (Hadjikhani et al. 1998), and a dorsal area adjacent to V3A, perhaps V7 (Mendola et al. 1999; Tootell et al. 1998a,b) or V3B (Smith et al. 1998). However, our retinotopy measurements were too noisy to map these areas with complete confidence in all subjects.

Similar results were evident across the eight subjects. Figure 4A plots fMRI response amplitudes (see METHODS) in each of several visual areas, averaged across subjects, for the two-plane/one-plane stimulus alternations. The fMRI responses were generally small in magnitude, but they could nevertheless be measured reliably. The mean responses were statistically significant in all visual areas except for MT+ ($P < 0.001$, 1-tailed t -tests of the unnormalized responses).

Area V3A was highly sensitive to stereoscopic depth. The responses were largest in V3A, smaller in V1, V2, and V3, and not significantly different from zero in MT+. The mean response in V3A tended to be larger than that in any of the other visual areas, although this was statistically significant only in comparison with V3 and MT+ ($P < 0.01$, 1-tailed t -tests on the unnormalized responses). The high sensitivity of area V3A was particularly evident after normalizing the responses. Figure 4*B* plots the responses from the two-plane/blank baseline scans. The baseline responses were largest in V1 and progressively smaller in the later visual areas (a 2-way ANOVA on the baseline responses showed significant effects of both subject, $P < 0.01$, and visual area, $P < 0.0001$). Figure 4*C* plots the normalized responses, i.e., after dividing the responses in the Fig. 4A by the respective baseline responses in Fig. 4B. The responses were normalized separately for each subject, before averaging across subjects, to compensate for the inter-subject differences in the baseline responses. V1 was distinguished by giving large responses in the baseline condition (Fig. 4*B*) but small responses in the two planes/one plane condition (Fig. 4A), so it had small normalized responses (Fig. 4C). In particular, alternating the two-plane stimulus with the one-plane stimulus evoked a modulation of V1 activity that was only 5% of that evoked by alternating the two-plane stimulus with a blank screen. V3A, by contrast, gave small responses in the baseline condition (Fig. 4*B*) but the largest responses when alternating between two planes and one plane (Fig. 4A), so it

had the largest (18%) normalized responses (Fig. 4C). The higher sensitivity of V3A to stereo disparity was evident in the normalized responses from all of the individual subjects.

Having established that cortical activity depends on stereoscopic depth, we proceeded to study this dependence in greater detail in two subjects (*BTB* and *DJH*) in the stereoacuity and upper depth limit experiments.

Stereoacuity

Psychophysical performance in the stereoacuity task is plotted in the pair of graphs on the left side of each panel in Fig. 5. Both subjects reliably distinguished the two-plane stimuli from the one-plane stimulus when the interplane disparities were greater than or equal to ± 0.5 arcmin. Below this disparity, performance dropped off; at half this disparity, d' was estimated to be < 1 , with the 95% confidence interval for percent correct no longer including the 75 percent correct point (assuming a binomial distribution for the behavioral responses). These psychophysical thresholds are consistent with reports in the literature for stimuli like ours (Stevenson et al. 1989).

Cortical activity as a function of interplane disparity is plotted on the *right side* of each panel in Fig. 5. The measured activity rose quickly as disparity increased. For *subject BTB*, the responses in all visual areas were statistically significant ($P < 0.05$, 1-tailed t -tests on the unnormalized responses) when the interplane disparity was ± 0.5 arcmin or more. For *subject DJH*, the responses in all areas were significant ($P < 0.05$, 1-tailed t -tests on the unnormalized responses) at ± 1 arcmin or more.

We again found that area V3A was remarkably sensitive to binocular disparity (Fig. 6). The responses in V3A were statistically significant ($P < 0.05$, 1-tailed t -tests on the unnormalized responses) in both subjects at the smallest interplane disparities tested (± 0.25 arcmin for *DJH* and ± 0.5 arcmin for

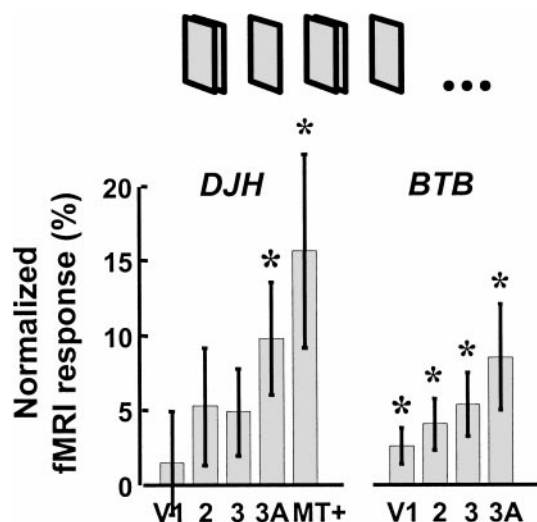


FIG. 6. Cortical activity for disparities near the stereoacuity threshold. Normalized responses (replotted from Fig. 5) at the smallest interplane disparities tested (± 0.5 arcmin for *BTB* and ± 0.25 arcmin for *DJH*). Significant activity was evident even for disparities at or below the stereoacuity thresholds. Areas V3A and MT+ were significantly more responsive than any of the other visual areas. Error bars represent 68% confidence intervals. * $P < 0.05$. ** $P < 0.01$ (1-tailed t -tests on unnormalized responses).

BTB). Even though *DJH* shows measurable V3A activity at a threshold-level disparity, it would be a mistake to say that V3A activity was more sensitive than the observer. The data show that V3A activity, averaged across a duration of many minutes, was more sensitive than the observer on a single trial. In fact, the variability in the fMRI measurements was probably dominated not by the noise that limited psychophysical performance, but rather by variability in hemodynamic response due to extraneous physiological factors (Biswal and Ulmer 1999; Biswal et al. 1997; Mitra et al. 1997; Stillman et al. 1995). It seems likely that V3A would show a smaller but still reliable activity at lower disparities still, if sufficient data could be collected to overcome measurement noise.

Off-horopter stereoacuity

Cortical activity covaried with psychophysical thresholds when the stereoacuity stimuli were positioned off the horopter. Figure 7 plots normalized responses for stimuli that alternated between two planes and one plane, for various interplane disparities and for various displacements in depth in front of or behind the fixation marker. When the interplane disparity was large enough, activity was generally greater for the two-plane stimuli than for one plane, even when all dots were in crossed (or all in uncrossed) disparity. However, the responses were small or absent when the interplane disparity was small (right-most set of bars for each subject). These small interplane disparities were chosen to be above the psychophysical stereoacuity threshold when the stimuli were presented at the horopter, but below threshold off the horopter (Blakemore 1970; Ogle 1953). On the horopter, these stimuli were perceptually different from the zero-disparity stimulus and evoked measurable responses (Fig. 5, $P < 0.05$ in V3A for *DJH* at ± 0.5 arcmin, $P < 0.01$ in all visual areas for *BTB* at ± 1 arcmin, 1-tailed t -tests on the unnormalized responses). Off the horopter, these stimuli were not perceptually distinguishable and did not evoke significant activity ($P > 0.35$ in all visual areas in both subjects, 1-tailed t -tests on the unnormalized responses).

Area V3A again showed the highest sensitivity to interplane disparity. In all five conditions for which interplane disparity was suprathreshold, the measured responses tended to be greatest in V3A and smallest in V1. For the two conditions with subthreshold disparities, there were no differences between areas because there was no measurable activity in any area.

Upper depth limits

Cortical activity again covaried with psychophysical performance in the upper disparity limit experiment, where the two-plane stimuli were alternated with a binocularly uncorrelated stimulus. As interplane disparity was increased, the two-plane stimuli became indistinguishable from the uncorrelated stimulus (Fig. 8, *left pair of graphs*). The modulation of cortical activity evoked by alternating the two-plane stimulus and the uncorrelated stimulus dropped to zero just before psychophysical performance dropped to chance levels (Fig. 8, *right pair of graphs*).

The zero-disparity stimulus evoked greater activity than the uncorrelated stimulus in all visual areas in *BTB* (leftmost data points, $P < 0.01$, 1-tailed t -test on the unnormalized re-

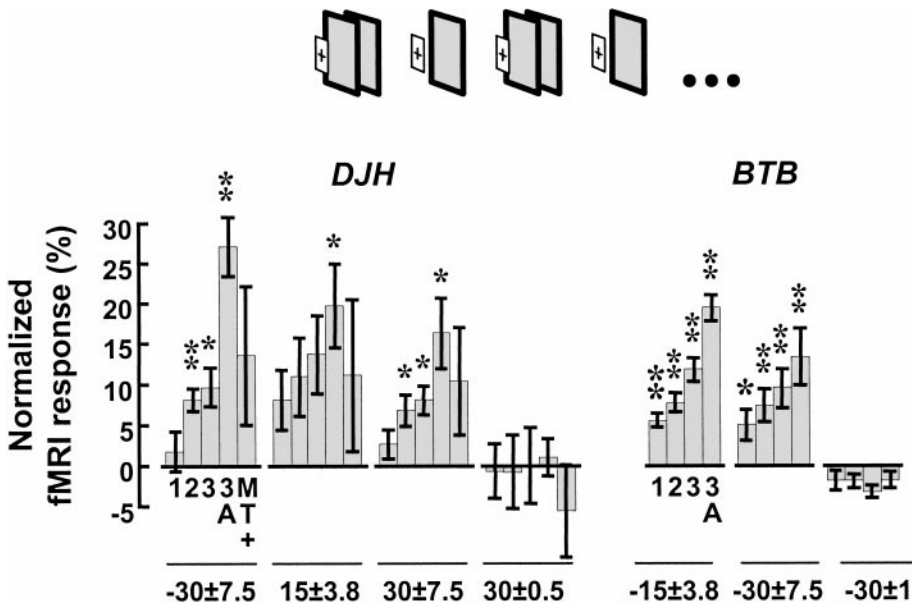


FIG. 7. Cortical activity in the off-horopter stereoacuity experiment. For each stimulus condition (4 for *DJH* and 3 for *BTB*), the 2-plane stimulus was alternated with a 1-plane stimulus at the same average nonzero disparity. When the interplane disparity was large enough, the 2-plane stimuli were perceptually distinguishable from 1 plane, and the cortical activity was generally greater than 0. However, when the interplane disparity was small (rightmost set of bars for each subject), the stimuli were not perceptually distinguishable, and the responses were small or absent. The stimulus conditions were, from left to right: for *DJH*, 30 ± 7.5 arcmin uncrossed, 15 ± 3.8 crossed, 30 ± 7.5 crossed, 30 ± 0.5 crossed; for *BTB*, 15 ± 3.8 arcmin uncrossed, 30 ± 7.5 uncrossed, and 30 ± 1 uncrossed. Error bars represent 68% confidence intervals. * $P < 0.05$. ** $P < 0.01$ (1-tailed *t*-tests on unnormalized responses).

sponses). The same trend was evident in *DJH*, but the responses were statistically significant at zero-disparity only in areas V2 and V3 ($P < 0.01$). As would be predicted from the stereoacuity data (Fig. 5), activity increased with disparity for small disparities. Once again the responses tended to be greatest in V3A and smallest in V1.

In an additional experiment (performed only on subject *BTB*

in 4 scans), a different spatial structure within the two-plane stimulus evoked similar levels of activity. This two-plane stimulus contained a corrugation in depth (horizontal stripes, each 3° tall, with dots in alternate stripes at ± 6 arcmin) instead of transparent planes, and was shown in alternation with the uncorrelated stimulus. Mean activity levels in V1, V2, V3, and V3A were almost identical to those in the most comparable condition using transparent planes (± 7.5 arcmin). Thus significant changes in the spatial structure of the stimulus had little or no effect on our measurements of the cortical responses.

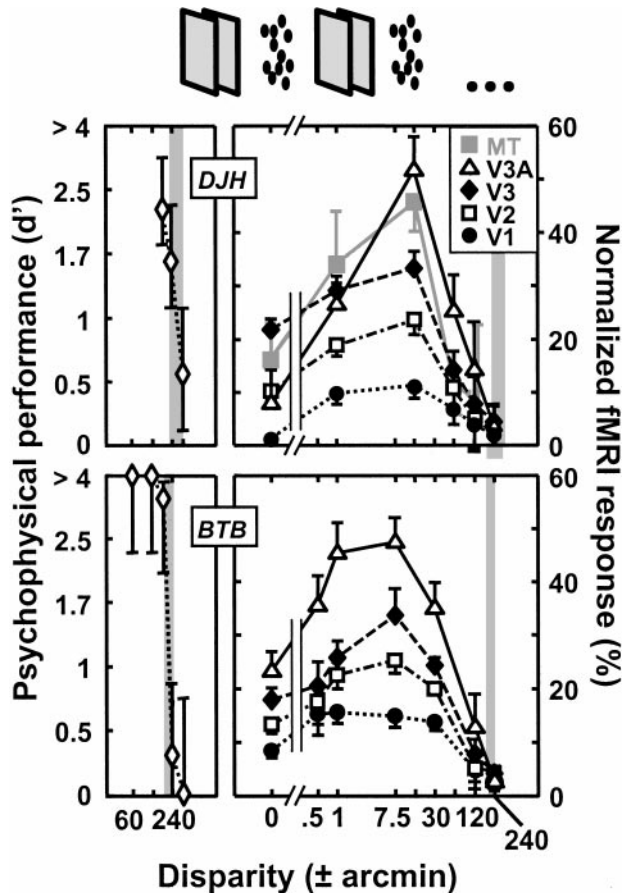


FIG. 8. Cortical activity and psychophysical performance in the upper depth limit experiment (same format as Fig. 5).

Attention control

Some of the difference in activity between the two-plane stimuli and the one-plane stimulus, or between two planes and the uncorrelated stimulus, might have had nothing to do with stereoscopic processing per se. Observers reported that the two-plane stimuli were more engaging, which could mean that they paid more attention during periods when the two-plane stimuli were displayed, resulting in greater cortical activity.

Although attention can strongly influence fMRI measurements of activity in visual cortex (Brefczynski and DeYoe 1999; Gandhi et al. 1999; Kastner et al. 1999; Ress et al. 2000; Somers et al. 1999; Tootell et al. 1998a; Watanabe et al. 1998), there is evidence that our measurements are not entirely the result of differential attention to the different stimulus conditions. First, the absolute response in V1 was larger than that in V3A when a two-plane stimulus was alternated with a blank screen, but V3A responded more than V1 when the two-plane stimuli were alternated with one plane. This interaction between cortical area and stimulus condition cannot be explained by a nonspecific, attention-related increase in response to the two-plane stimuli. Second, to the extent that attention evokes a multiplicative change in the gain of cortical responses (Hillyard et al. 1998; McAdams and Maunsell 1999; Treue and Martinez Trujillo 1999), these attentional influences were mitigated by our normalization procedure (dividing by the baseline responses). Third, neural responses continued to increase with interplane disparity (Fig. 5), even after the two-plane stimuli were easily discriminated from one plane. Likewise,

responses in the upper depth limit experiment started to drop well before the two-plane stimuli became indiscriminable from the uncorrelated stimulus (Fig. 8). These findings are consistent with a previous observation that the amplitudes of evoked potentials increased with disparity for a single random-dot plane alternating in depth (Norcia et al. 1985).

Nonetheless, we performed an additional experiment aimed to explicitly control subjects' attention by having them perform a demanding depth discrimination task throughout each scan (see METHODS). The results, plotted in Fig. 9, suggest that the measured cortical signals reflect both sensory and attentional influences. Figure 9A plots the responses from scans in which subjects performed the depth discrimination task, and Fig. 9B plots the responses when subjects viewed similar stimuli without performing the task. The responses are smaller in Fig. 9A than Fig. 9B, suggesting that exogenous attention to the stereoscopic two-plane stimulus during passive fixation contributed to our measured responses. Even so, both data sets show the same pattern across visual areas. Whether or not the task was performed, 1) the normalized responses were smallest in V1 and progressively larger in V2, V3, and V3A; 2) the responses were statistically significant in each of several visual areas, in both subjects (*DJH* task: V2, V3, V3A; *BTB* task: V1, V2, V3A; *DJH* no task: V1, V2, V3, V3A; *BTB* no task: V3A; $P < 0.5$, 1-tailed t -tests on the unnormalized responses); and 3) the responses in V3A were significantly larger than those in any of the other visual areas, in both subjects ($P < 0.5$, 1-tailed t -tests on the unnormalized responses).

Consistent with the results from our other experiments, certain cortical regions responded more strongly to the two-plane stimulus (i.e., containing stereoscopic depth) than the one-plane stimulus, whether or not subjects performed the depth discrimination task. However, there were adjacent subregions in several visual areas that responded more strongly to one-plane than two-planes only when subjects were performing the task. These subregions did not exhibit any preference for one stimulus over the other without the task. Further experiments will have to be performed to determine why this was the case.

If it is the very nature of depth-containing stimuli to compel greater attention, then of course we cannot dissociate bot-

tom-up stimulus-evoked responses from top-down attentional effects, because the latter would be driven directly by the former. An attentional effect of this sort would have to vary parametrically in size with disparity to account for the data. We do not suggest that this is the case, but we must admit that it is a possibility.

Response saturation control

The fMRI responses evoked by our disparity manipulations were small relative to the large responses evoked when alternating the random-dot stimuli with a blank screen. In V1, for example, the response amplitude was 0.13 in the two-plane/one-plane scans (Fig. 4A) as compared with 2.6 in the two-plane/blank scans (Fig. 4B). This led us to be concerned about response saturation. If the hemodynamic response saturates (levels off) with increases in neuronal activity, then the presence/absence of the random-dot stimuli might evoke a nearly maximum fMRI response in V1, thereby leaving very little headroom to reveal any additional increment in neuronal activity as a function of stimulus disparity.

We performed a control experiment to test for effects of response saturation, using low contrast stimuli. The results, plotted in Fig. 10, demonstrate that our results are not confounded by response saturation. Even at low contrasts, the responses were statistically significant in each of several visual areas, in all three subjects (*DJH*: all areas except V1; *BTB*: all areas except MT+; *ACH*: V3, V3A; $P < 0.5$, 1-tailed t -tests on the unnormalized responses). Even at low contrasts, the responses in V3A were significantly larger than those in any of the other visual areas in subjects *DJH* and *BTB*, and the V3A responses were larger than those in all areas except MT+ in subject *ACH* ($P < 0.5$, 1-tailed t -tests on the unnormalized responses).

Critically, the low contrast stimuli avoided saturation by leaving plenty of headroom available for larger responses. The V1 responses in the low contrast baseline scans (Fig. 10B), averaged across the three subjects, were 58% as large as those measured at high contrast (culled from the data plotted in Fig. 4). This is consistent with previous fMRI measurements of the contrast dependence of V1 activity (Boynton et al. 1996, 1999; Demb et al. 1998; Goodyear and Menon 1998; Tootell et al. 1995). The change from high to low contrast caused the V1 responses in the two-plane/one-plane scans and the two-plane/blank scans to change by about the same scale factor, so that the normalized V1 responses were roughly the same for low (Fig. 10C) and high (Fig. 4C) contrasts. The high contrast two-plane/blank scans evoked progressively smaller responses in V1, V2, V3, V3A, and MT+, respectively; however, the low contrast responses were similar across these areas (compare Figs. 4B and 10B). MT+ responses appear to be positive in the low contrast experiment (Fig. 10A) and near-zero in the high contrast experiment (Fig. 4A), but in fact the data plotted in Figs. 10 and 4 are not directly comparable because the Fig. 4 data were collected from a larger group of subjects. Two of the three subjects that were included in both experiments had similar MT+ responses in the two experiments. The third subject had larger MT+ responses at low contrast ($P < 0.05$). Indeed MT+ responses were generally highly variable across subjects and experiments.

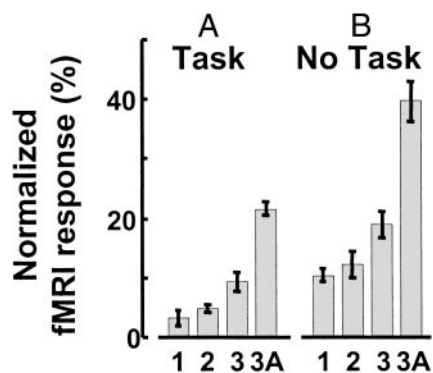


FIG. 9. Cortical activity in our experiments was not dominated by attentional influences. A: normalized responses, averaged across scans in which 2 subjects performed depth discrimination judgements on stimuli that periodically alternated between large and small interplane disparities (see METHODS). B: normalized responses from scans of the same stimulus conditions, but without performing the depth discrimination task. Error bars represent 68% confidence intervals for the mean responses of the 2 subjects (not confidence intervals for the population mean).

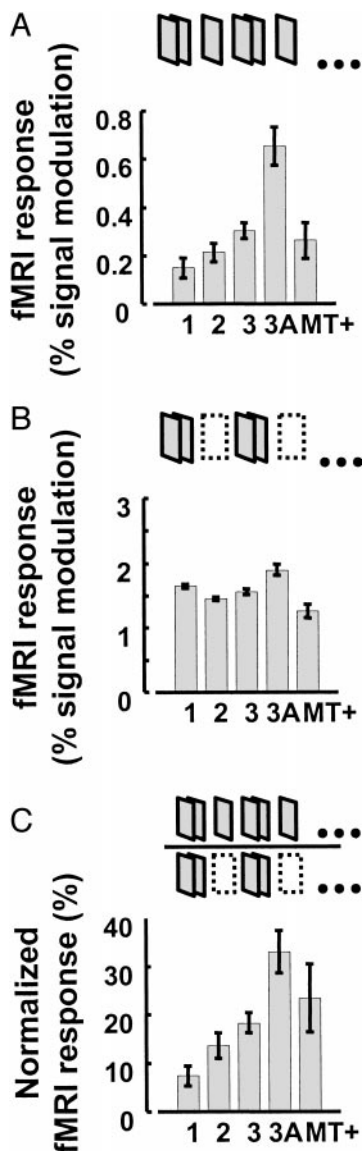


FIG. 10. Cortical activity in our experiments was not confounded by response saturation. A–C: fMRI responses to low contrast stimuli (same format as Fig. 3), averaged across 3 subjects. Error bars represent 68% confidence intervals for the mean of the 3 subjects (not confidence intervals for the population mean).

Eye movement control

Differences in eye movements between conditions could potentially confound the interpretation of some of our results. A tendency to make more fixational, vergence, or pursuit eye movements while viewing the two plane stimuli might have been sufficient to modulate the fMRI signal. Specifically, eye movements might have evoked differentially larger responses in some areas (e.g., V3A and MT+) with a greater proportion of motion-sensitive neurons than other visual areas.

We believe, however, that our measurements are not confounded by eye movements. First, the bulk of the data were collected with balanced disparity (crossed and uncrossed) to avoid just this problem; it is known that crossed and uncrossed disparities cancel each other during automatic vergence eye movements (Mallot et al. 1996). Second, the Nonius lines in

the stimuli were large and salient, and their position was easy to monitor subjectively. Third, because the dot patterns were updated at 4 Hz, it seems likely that the cortical activity induced by small versional eye movements would be insignificant relative to that induced by the motion energy present in the stimuli at all times. Fourth, *subjects DJH, BTB, and ACH* have previously shown the ability to accurately fixate dynamic stimuli (Huk and Heeger 2000).

As a further precaution against differences due eye movement patterns, we measured the eye movements of *subjects DJH* and *BTB* while they viewed a subset of the stimulus conditions, in the same blocked design as in the fMRI experiments. Inspection of the traces showed that across subjects and conditions, eye position was steady to within $\pm 0.25^\circ$ of fixation.

DISCUSSION

The main result of this study is that activity in early visual cortex covaries with stereoscopic depth perception. Perceptually, subjects cannot distinguish a one-plane stimulus from a two-plane stimulus when the interplane disparity is too small. Likewise, subjects cannot distinguish a two-plane stimulus from a binocularly uncorrelated stimulus when the interplane disparity is too large. Cortical activity in each of the studied visual areas followed the same pattern; activity first increased with disparity for interplane disparities from 0 to ~ 15 arcmin (Fig. 5), and then decreased with disparity for interplane disparities greater than ~ 30 arcmin (Fig. 8). Both perception and cortical activity depended on where the stimuli were placed in depth relative to fixation, that is, relative to the horopter. On the horopter, a small interplane disparity was perceptually detectable and evoked a measurable increase in cortical activity (Fig. 6). Off the horopter, a slightly larger interplane disparity was undetectable and did not evoke an increase in cortical activity (Fig. 7). Thus activity in visual cortex, pooled across a very large number of neurons, rises quickly in the vicinity of psychophysical threshold.

We also found that area V3A was highly sensitive to binocular disparity, exhibiting clear responses right down to the neighborhood of psychophysical threshold (Fig. 6). V3A was generally the most responsive of the five studied visual areas. V2 and V3 gave intermediate normalized responses, and V1 generally gave the smallest normalized responses. MT+ responses were highly variable across subjects and experiments; MT+ appeared to be sensitive to binocular disparity in some experiments (e.g., Fig. 6, *subject DJH*; Fig. 10), but not in other experiments (e.g., Fig. 4).

Possible interpretations

The interpretation of fMRI measurements is hampered by our lack of understanding about how they relate to neural activity. The available evidence suggests that fMRI responses are correlated with average neural activity (Heeger et al. 1999, 2000; Logothetis et al. 2001; Rees et al. 2000a; Seidemann et al. 1999; Wandell et al. 1999). But even so, the interpretation of our fMRI data are limited by two issues. First, stereoscopic depth judgments involve multiple processes. Second, our fMRI measurements combined the activity indiscriminately of many neurons in each cortical area, whereas it is unlikely that sub-

jects monitored total neuronal activity to distinguish two-plane from one-plane stimuli.

No fewer than six processes are active during stereoscopic vision, any of which could in principle contribute to changes in neural activity that we observed as a function of disparity. First, and most obvious, is the computation (and neural representation) of the absolute disparities of the dots in the stimulus. The relatively large responses we observed in V3A might result from the presence of neurons that are similar to disparity-responsive V1 neurons, but in greater numbers per unit volume of cortex. Second is the explicit computation of relative disparity. The finest stereoacuity judgments are generated psychophysically only by stimuli that contain relative disparity information (Kumar and Glaser 1992; Westheimer 1979). The two-plane stimuli in our experiments afforded the extraction of relative disparities. The relatively high sensitivity we observed in area V3A would be expected if neurons in this area represent relative disparity. Third is the spread of disparity information to initiate depth filling-in. The dots in our stimuli appear to lie on surfaces, which suggests a process that “fills in” the depth for the blank spaces between the dots. This process might involve more neural processing for two surfaces than one surface. A fourth neural process is segmentation based on disparity (Parker and Yang 1989; Stevenson et al. 1989; Westheimer 1986). At intermediate interplane disparities (roughly ± 1 arcmin to $\pm 1.5^\circ$) the two-plane stimulus segregates perceptually into two distinct surfaces at different depths. Fifth is calibration of disparity to estimate depth. For two planes, an additional computation is needed to determine the depth between them, which depends on the visual system’s estimate of their distance from the observer (Howard and Rogers 1995; Wallach and Zuckerman 1963). Sixth, some stimuli may, by virtue of the percept they create, compel attention-related or other top-down activity in early visual areas. Because we did not explicitly control each of these neural processes related to stereoscopic vision, we cannot distinguish between them as causes for the observed changes in fMRI activity. Note, however, that the same interpretational ambiguities would apply in an electrophysiology experiment.

The fMRI signal effectively integrates activity within a volume of cortex containing millions of neurons. fMRI cannot therefore distinguish a high firing rate in each of a few neurons from a low firing rate in many neurons. Nor can it reveal an increased firing rate in a subpopulation of neurons when offset by a decreased firing rate in other neurons nearby. The inverted-U fMRI data of Fig. 8 might be predicted from a detailed description of the neural population (as we do for area V1 in *Comparison with V1 electrophysiology*), but inference in the other direction is impossible.

Despite these complications, the current results provide a useful platform for further imaging research on stereopsis, and constrain models of the neural processing that support stereoscopic vision in humans. For example, a straightforward implementation of the Lehky and Sejnowski (1990) neural model of stereoacuity predicted greater average activity in cortical area V1 for the one-plane stimulus than for the two-plane stimulus, in disagreement with our results. We next consider the relationship between the fMRI signal and single-unit physiology in the context of our data.

Comparison with V1 electrophysiology

The responses of individual macaque neurons to disparity are best characterized for area V1. Given the published literature, it is plausible but not obvious that average V1 firing rates would increase with interplane disparity above the stereoacuity threshold, then decrease as interplane disparity approaches the upper depth limit. Prince et al. (2000) found significant changes in the firing patterns of single V1 cortical neurons when single-plane random dot stimuli were altered in disparity by as little as 0.6–1.2 arcmin, corresponding well to the smallest interplane disparities of 0.5–1 (± 0.25 to ± 0.5) arcmin in our two-plane stimuli. In V1 a large number of neurons are tuned for zero disparity (Poggio et al. 1988). These neurons would fire maximally to the (single plane) zero-disparity stimulus, and less to (2 plane) stimuli with nonzero interplane disparities. Other V1 neurons fire maximally to near disparities or far disparities. These neurons could respond best to two-plane stimuli with appropriate interplane disparities and less to the (single plane) zero-disparity stimulus. The pooled activity, as measured with fMRI, depends on the relative sizes of these two effects, i.e., the relative responsiveness and the relative number of neurons in V1 with different disparity tuning. That V1 responded more strongly to the two-plane stimulus than to the one-plane stimulus (Figs. 4 and 5) therefore suggests that the mean activity of V1 neurons is a bimodal function of absolute retinal disparity. That the fMRI response falls off at large interplane disparities suggests that the local maxima are < 60 arcmin apart. That small interplane disparities evoke fMRI responses suggests that the central trough in the bimodal response function is narrow and centered at zero disparity.

Prince et al. (2001b) characterized disparity tuning for 180 disparity-selective neurons in macaque V1. These data permit a post hoc test of the prediction that primate V1 neurons fire more, on average, to nonzero than to zero disparity. Although the 180 neurons’ collective ability to detect a small change in disparity was unimodally distributed near zero disparity (Prince et al. 2001a), we report here the surprising discovery that average firing rate was bimodal as a function of disparity (Fig. 11). This finding was robust, that is, it did not depend on just a few neurons within the sample. We performed a bootstrap analysis of the Prince et al. (2001a) data by 1) repeatedly summing the responses of 180 neurons drawn at random with replacement, to create a bootstrap sample of 1,000 curves, 2) subtracting out baseline differences between the curves (baseline standard deviation, 405 spikes/s), 3) separately ordering

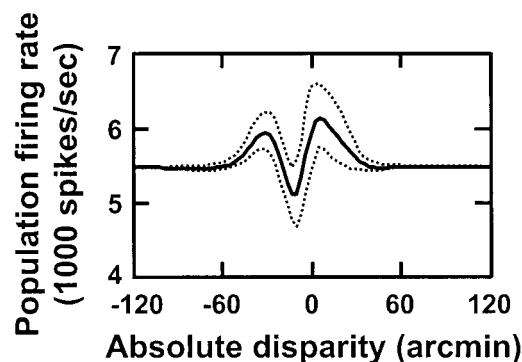


FIG. 11. Total activity (spikes/s) as a function of absolute disparity for the 180 macaque V1 neurons characterized by Prince et al. (2001b). Dotted curves, 95% confidence bounds. Crossed disparity is negative.

the 1,000 values from these curves at each disparity, and 4) plotting the 2.5th and 97.5th percentile at each disparity (dotted curves in Fig. 11). Of 1,000 bootstrap sample curves, only 8 failed to show a central trough between 2 peaks. Figure 11 thus confirms the prediction of bimodality and that the local maxima are spaced <60 arcmin apart. There were a number of differences between experimental protocols in the human fMRI and monkey single-unit experiments, including differences in the stimulus parameters, but the sample of 180 neurons was selected on the basis that they showed statistically significant changes in firing when stimulus disparity was altered, so we suspect that bimodality characterizes the population of V1 disparity-selective neurons as a whole.

Figure 11 also shows that the prediction of a narrow trough at zero disparity was not confirmed. Instead, the trough was relatively broad and was centered at 10–15 arcmin crossed disparity. Thus the response of these neurons to absolute disparity cannot fully explain the fMRI responses we observed in V1. One explanation for this failure is that the fMRI response to small interplane disparities may have been due to neurons coding central vision, where stereoacuity is highest (McKee 1983; Rawlings and Shipley 1969), whereas neurons in the macaque sample coded a range of eccentricities. A second explanation is that some component of the fMRI response in V1 may be due to factors other than absolute disparity per se (see *Possible interpretations*). This view is supported by the fMRI responses we observed in V1 using off-horopter stimuli (Fig. 7, *subject BTB*) and the reduced response of V1 when a task was used to control attentional affects (Fig. 9).

As with disparity, it is plausible but not obvious that average V1 firing rates would be larger for correlated stimuli than for binocularly uncorrelated stimuli, due to binocular facilitation (Freeman and Ohzawa 1990). Complex cells in V1 act essentially as correlation detectors (Anzai et al. 1999; Fleet et al. 1996; Ohzawa et al. 1990) and could therefore account for the greater activity evoked by our correlated one- and two-plane stimuli, as compared with our uncorrelated stimulus. On the other hand, the uncorrelated stimulus ought to impinge on the receptive fields of more cortical neurons than do the correlated stimuli. Thus the greater cortical activity observed for correlated stimuli probably reflects a decrease in the total number of neurons activated, together with a more than compensatory increase in the response of those neurons. Average neural activity for an uncorrelated stimulus is predicted in Fig. 11 by the asymptotes on either side of the wiggle, as these asymptotes give the response to stimuli with very large disparities, which is expected to equal the uncorrelated response. Figure 8 (*rightmost data*) shows that large-disparity and uncorrelated fMRI responses were indeed the same.

Stereo pathway beyond V1

Neurophysiological studies have shown that there is a generally widespread distribution of disparity-selective neurons throughout the striate and extrastriate cortex of nonhuman primates (Burkhalter and Van Essen 1986; Maunsell and Van Essen 1983; Poggio 1995). Little has been done to divide these neurons into classes that can be more specifically associated with identified visual areas. Nonetheless, it is known that there is a columnar organization for disparity in macaque areas V2 (Hubel and Livingstone 1987; Hubel and Wiesel 1970; Peter-

hans and von der Heydt 1993; Roe and Ts'o 1995) and MT (DeAngelis and Newsome 1999), and also that binocular facilitation of neuronal responses may vary from area to area when tested with zero-disparity stimuli (Zeki 1978, 1979). These observations are clearly relevant to understanding the neural processing that supports stereoscopic depth perception, although they do not nearly provide an account of the process.

Poggio et al. (1988) examined the disparity selectivity of neurons in macaque visual cortex in some detail. Two of their findings may be particularly relevant to the interpretation of our own data. First, they found that the ratio of disparity-responsive to disparity-unresponsive neurons was 1:1 for V1, 2:1 for V2, and 4:1 in a region that probably was V3-V3A. This is qualitatively consistent with differences in responses we observed across these visual areas: we also observed significantly larger responses to stereoscopic stimuli in areas beyond V1 than in V1 itself. However, the V3-V3A neurons they encountered had receptive fields centered more peripherally than their V1 neurons, so while perhaps suggestive, we cannot draw an ironclad connection between those data and ours. Second, they found that in V1 many neurons were tuned to near-zero disparities, but that in V3-V3A almost all neurons were tuned near or far. This finding is also consistent with our data, but again the difference in eccentricities in those samples makes it logically difficult to predict our responses from their data. In addition, there are known differences between visual processing in monkey and human V3A (Tootell et al. 1997).

Since areas V3 and V3A have been associated with stereoscopic depth signals in earlier single-unit recording experiments (Poggio et al. 1988), a consistent interpretation of the specific fMRI signal observed in V3A is that it could arise from a concentration of neurons sensitive to relative disparity; if the neurons carry signals about relative disparity, then they would respond specifically to the presence of the interplane disparity in our two-plane stimulus. Further experiments in the extrastriate cortex will be necessary for testing this particular interpretation. Regardless of whether this speculation is correct, the present results add considerably to the case that V3A may be relatively specialized for stereoscopic processing.

We thank H. Baseler, R. Dougherty, A. Huk, R. Khan, C. Tyler, and A. Wade for serving as subjects; G. H. Glover (and the Richard M. Lucas Center for Magnetic Resonance Spectroscopy and Imaging, supported by a National Center for Research Resources grant) for technical support; and S. Prince and B. Cumming for providing single unit data.

This research was supported by National Eye Institute Grant R01-EY-12741 to D. J. Heeger, an Alfred P. Sloan Research Fellowship to D. J. Fleet, a grant from the Wellcome Trust (UK) to A. J. Parker, and National Research Service Award Postdoctoral Fellowship F32-EY-06899 to B. T. Backus.

REFERENCES

- AGUIRRE GK, ZARAHN E, AND D'ESPOSITO M. The variability of human, BOLD hemodynamic responses. *Neuroimage* 8: 360–369, 1998.
- ANZAI A, OHZAWA I, AND FREEMAN RD. Neural mechanisms for processing binocular information. II. Complex cells. *J Neurophysiol* 82: 909–924, 1999.
- BARLOW HB, BLAKEMORE C, AND PETTIGREW JD. The neural mechanism of binocular depth discrimination. *J Physiol (Lond)* 193: 327–342, 1967.
- BISWAL BB AND ULMER JL. Blind source separation of multiple signal sources of fMRI data sets using independent component analysis. *J Comput Assist Tomogr* 23: 265–271, 1999.
- BISWAL BB, VAN KYLEN J, AND HYDE JS. Simultaneous assessment of flow and BOLD signals in resting-state functional connectivity maps. *NMR Biomed* 10: 165–170, 1997.

- BLAKEMORE C. The range and scope of binocular depth discrimination in man. *J Physiol (Lond)* 211: 599–622, 1970.
- BOYNTON GM, DEMB JB, GLOVER GH, AND HEEGER DJ. Neuronal basis of contrast discrimination. *Vision Res* 39: 257–269, 1999.
- BOYNTON GM, ENGEL SA, GLOVER GH, AND HEEGER DJ. Linear systems analysis of functional magnetic resonance imaging in human V1. *J Neurosci* 16: 4207–4221, 1996.
- BRADDICK OJ AND ATKINSON J. Some recent findings on the development of human binocularity: a review. *Behav Brain Res* 10: 141–150, 1983.
- BREPCZYNSKI JA AND DEYOE EA. A physiological correlate of the 'spotlight' of visual attention. *Nature Neurosci* 2: 370–374, 1999.
- BURKHALTER A AND VAN ESSEN DC. Processing of color, form and disparity information in visual areas VP and V2 of ventral extrastriate cortex in the macaque monkey. *J Neurosci* 6: 2327–2351, 1986.
- CUMMING BG AND PARKER AJ. Responses of primary visual cortical neurons to binocular disparity without depth perception. *Nature* 389: 280–283, 1997.
- CUMMING BG AND PARKER AJ. Binocular neurons in V1 of awake monkeys are selective for absolute, not relative, disparity. *J Neurosci* 19: 5602–5618, 1999.
- CUMMING BG AND PARKER AJ. Local disparity not perceived depth is signaled by binocular neurons in cortical area V1 of the macaque. *J Neurosci* 20: 4758–4767, 2000.
- DEANGELIS GC AND NEWSOME WT. Organization of disparity-selective neurons in macaque area MT. *J Neurosci* 19: 1398–1415, 1999.
- DEMB JB, BOYNTON GM, AND HEEGER DJ. Functional magnetic resonance imaging of early visual pathways in dyslexia. *J Neurosci* 18: 6939–6951, 1998.
- DEYOE EA, CARMAN GJ, BANDETTINI P, GLICKMAN S, WIESER J, COX R, MILLER D, AND NEITZ J. Mapping striate and extrastriate visual areas in human cerebral cortex. *Proc Natl Acad Sci USA* 93: 2382–2386, 1996.
- EFRON B AND TIBSHIRANI RJ. *An Introduction to the Bootstrap*. New York: Chapman and Hall, 1993.
- ENGEL SA, GLOVER GH, AND WANDELL BA. Retinotopic organization in human visual cortex and the spatial precision of functional MRI. *Cereb Cortex* 7: 181–192, 1997.
- ENGEL SA, RUMELHART DE, WANDELL BA, LEE AT, GLOVER GH, CHICHILNISKY EJ, AND SHADLEN MN. fMRI of human visual cortex. *Nature* 369: 525, 1994.
- FIORENTINI A AND MAFFEI L. Electrophysiological evidence for binocular disparity detectors in human visual system. *Science* 169: 208–209, 1970.
- FLEET DJ, WAGNER H, AND HEEGER DJ. Neural encoding of binocular disparity: energy models, position shifts and phase shifts. *Vision Res* 36: 1839–1857, 1996.
- FREEMAN RD AND OHZAWA I. On the neurophysiological organization of binocular vision. *Vision Res* 30: 1661–1676, 1990.
- GANDHI SP, HEEGER DJ, AND BOYNTON GM. Spatial attention affects brain activity in human primary visual cortex. *Proc Natl Acad Sci USA* 96: 3314–3319, 1999.
- GLOVER GH. Simple analytic spiral K-space algorithm. *Magn Reson Med* 42: 412–415, 1999.
- GLOVER GH AND LAI S. Self-navigated spiral fMRI: interleaved versus single-shot. *Magn Reson Med* 39: 361–368, 1998.
- GONZALEZ F AND PEREZ R. Neural mechanisms underlying stereoscopic vision. *Prog Neurobiol* 55: 191–224, 1998.
- GOODYEAR BG AND MENON RS. Effect of luminance contrast on BOLD fMRI response in human primary visual areas. *J Neurophysiol* 79: 2204–2207, 1998.
- GREEN DM AND SWETS JA. *Signal Detection Theory and Psychophysics*. New York: Krieger, 1966.
- GULYAS B AND ROLAND PE. Binocular disparity discrimination in human cerebral cortex: functional anatomy by positron emission tomography. *Proc Natl Acad Sci USA* 91: 1239–1243, 1994.
- HADJIKHANI N, LIU AK, DALE AM, CAVANAGH P, AND TOOTELL RB. Retinotopy and color sensitivity in human visual cortical area V8. *Nature Neurosci* 1: 235–241, 1998.
- HEEGER DJ. Normalization of cell responses in cat striate cortex. *Vis Neurosci* 9: 181–197, 1992.
- HEEGER DJ, BOYNTON GM, DEMB JB, SEIDEMANN E, AND NEWSOME WT. Motion opponency in visual cortex. *J Neurosci* 19: 7162–7174, 1999.
- HEEGER DJ, HUK AC, GEISLER WS, AND ALBRECHT DG. Spikes versus BOLD: what does neuroimaging tell us about neuronal activity? *Nature Neurosci* 3: 631–633, 2000.
- HILLYARD SA, VOGEL EK, AND LUCK SJ. Sensory gain control (amplification) as a mechanism of selective attention: electrophysiological and neuroimaging evidence. *Philos Trans R Soc Lond B Biol Sci* 353: 1257–1270, 1998.
- HINKLE DA AND CONNER CE. Disparity tuning in macaque area V4. *Neuroreport* 12: 356–369, 2001.
- HOWARD IP AND ROGERS BJ. *Binocular Vision and Stereopsis*. New York: Oxford, 1995, p. 149–602, 456–459.
- HUBEL DH AND LIVINGSTONE MS. Segregation of form, color, and stereopsis in primate area 18. *J Neurosci* 7: 3378–3415, 1987.
- HUBEL DH AND WIESEL TN. Stereoscopic vision in macaque monkey. Cells sensitive to binocular depth in area 18 of the macaque monkey cortex. *Nature* 225: 41–42, 1970.
- HUK AC AND HEEGER DJ. Task-related modulation of visual cortex. *J Neurophysiol* 83: 3525–3536, 2000.
- KASTNER S, PINSK MA, DE WEERD P, DESIMONE R, AND UNGERLEIDER LG. Increased activity in human visual cortex during directed attention in the absence of visual stimulation. *Neuron* 22: 751–761, 1999.
- KHAN RM, BOYNTON GM, FLEET DJ, AND HEEGER DJ. Neural basis of stereo depth perception measured with fMRI. *Invest Ophthalmol Vis Sci Abstr Book* 38: S625, 1997.
- KUMAR T AND GLASER DA. Depth discrimination of a line is improved by adding other nearby lines. *Vision Res* 32: 1667–1676, 1992.
- LEHYK SR AND SEINOWSKI TJ. Neural model of stereoacuity and depth interpolation based on a distributed representation of stereo disparity. *J Neurosci* 10: 2281–2299, 1990.
- LOGOTHETIS NK, PAULS J, AUGATH M, TRINATH T, AND OELTERMANN A. Neurophysiological investigation of the basis of the fMRI signal. *Nature* 412: 150–157, 2001.
- MALLOT HA, ROLL A, AND ARNDT PA. Disparity-evoked vergence is driven by interocular correlation. *Vision Res* 36: 2925–2937, 1996.
- MAUNSELL JH AND VAN ESSEN DC. Functional properties of neurons in middle temporal visual area of the macaque monkey. II. Binocular interactions and sensitivity to binocular disparity. *J Neurophysiol* 49: 1148–1167, 1983.
- MCADAMS CJ AND MAUNSELL JHR. Effects of attention on orientation-tuning functions of single neurons in macaque cortical area V4. *J Neurosci* 19: 431–441, 1999.
- MCKEE SP. The spatial requirements for fine stereoacuity. *Vision Res* 23: 191–198, 1983.
- MENDOLA JD, DALE AM, FISCHL B, LIU AK, AND TOOTELL RB. The representation of illusory and real contours in human cortical visual areas revealed by functional magnetic resonance imaging. *J Neurosci* 19: 8560–8572, 1999.
- MITRA PP, OGAWA S, HU X, AND UGURBIL K. The nature of spatiotemporal changes in cerebral hemodynamics as manifested in functional magnetic resonance imaging. *Magn Reson Med* 37: 511–518, 1997.
- NAKADOMARI S, KITAHARA K, KAMADA Y, YOSHIDA K, SAITO M, AND MIYAUCHI S. The cuneus plays an important role in stereoscopic vision: a neuropsychological and fMRI study. *Invest Ophthalmol Vis Sci Abstr Book* 40: S819, 1999.
- NESTARES O AND HEEGER DJ. Robust multiresolution alignment of MRI brain volumes. *Magn Reson Med* 43: 705–715, 2000.
- NIKARA T, BISHOP PO, AND PETTIGREW JD. Analysis of retinal correspondence by studying receptive fields of binocular single units in cat striate cortex. *Exp Brain Res* 6: 353–372, 1968.
- NOLL DC, COHEN JD, MEYER CH, AND SCHNEIDER W. Spiral K-space MR imaging of cortical activation. *J Magn Reson Imaging* 5: 49–56, 1995.
- NORCIA AM, SUTTER EE, AND TYLER CW. Electrophysiological evidence for the existence of coarse and fine disparity mechanisms in human. *Vision Res* 25: 1603–1611, 1985.
- NORCIA AM AND TYLER CW. Temporal frequency limits for stereoscopic apparent motion processes. *Vision Res* 24: 395–401, 1984.
- OGLE KN. Precision and validity of stereoscopic depth perception from double images. *J Opt Soc Am* 43: 906–913, 1953.
- OHZAWA I, DEANGELIS GC, AND FREEMAN RD. Stereoscopic depth discrimination in the visual cortex: neurons ideally suited as disparity detectors. *Science* 249: 1037–1041, 1990.
- OHZAWA I, SCLAR G, AND FREEMAN RD. Contrast gain control in the cat's visual system. *J Neurophysiol* 54: 651–667, 1985.
- PARKER AJ, CUMMING BG, AND DODD JV. Binocular neurons and the perception of depth. In: *The New Cognitive Neurosciences*, edited by Blakemore C and Movshon JA. Cambridge, MA: MIT Press, 2000.
- PARKER AJ AND YANG Y. Spatial properties of disparity pooling in human stereo vision. *Vision Res* 29: 1525–1538, 1989.

- PETERHANS E AND VON DER HEYDT R. Functional organization of area V2 in the alert macaque. *Eur J Neurosci* 5: 509–524, 1993.
- PETTIGREW JD, NIKARA T, AND BISHOP PO. Binocular interaction on single units in cat striate cortex: simultaneous stimulation by single moving slit with receptive fields in correspondence. *Exp Brain Res* 6: 391–410, 1968.
- POGGIO GF. Mechanisms of stereopsis in monkey visual cortex. *Cereb Cortex* 5: 193–204, 1995.
- POGGIO GF, GONZALEZ F, AND KRAUSE F. Stereoscopic mechanisms in monkey visual cortex: binocular correlation and disparity selectivity. *J Neurosci* 8: 4531–4550, 1988.
- PRINCE SJ, CUMMING BG, AND PARKER AJ. Range and mechanism of encoding of horizontal disparity in macaque V1. *J Neurophysiol*. In press, 2001a.
- PRINCE SJ, POINTON AD, CUMMING BG, AND PARKER AJ. The precision of single neuron responses in cortical area V1 during stereoscopic depth judgments. *J Neurosci* 20: 3387–3400, 2000.
- PRINCE SJ, POINTON AD, CUMMING BG, AND PARKER AJ. Quantitative analysis of the responses of V1 neurons to horizontal disparity in dynamic random dot stereograms. *J Neurophysiol*. In press, 2001b.
- PTITO A, ZATORRE RJ, PETRIDES M, FREY S, ALIVISATOS B, AND EVANS AC. Localization and lateralization of stereoscopic processing in the human brain. *Neuroreport* 4: 1155–1158, 1993.
- RAWLINGS SC AND SHIPLEY T. Stereoscopic acuity and horizontal angular distance from fixation. *J Opt Soc Am* 59: 991–993, 1969.
- REES G, FRISTON K, AND KOCH C. A direct quantitative relationship between the functional properties of human and macaque V5. *Nature Neurosci* 3: 716–723, 2000a.
- REES G, FRISTON K, AND KOCH C. A direct quantitative relationship between the functional properties of human and macaque V5. *Nature Neurosci* 3: 716–723, 2000b.
- RESS D, BACKUS BT, AND HEEGER DJ. Activity in primary visual cortex predicts performance in a visual detection task. *Nature Neurosci* 3: 940–945, 2000.
- ROE AW AND TS'O DY. Visual topography in primate V2: multiple representation across functional stripes. *J Neurosci* 15: 3689–3715, 1995.
- RUTSCHMANN R AND GREENLEE M. Human cortical areas responding to disparity: an fMRI study. *Perception* 28 (Abstract Suppl.): 134, 1999.
- SAWYER-GLOVER A AND GLOVER G. fMRI of the motor cortex: comparison of EPI and spiral pulse sequences. *Proc SMRT Seventh Annu Meet, Sydney, Australia*, 1998, p. 69.
- SEIDEMANN E, POIRSON AB, WANDELL BA, AND NEWSOME WT. Color signals in area MT of the macaque monkey. *Neuron* 24: 911–917, 1999.
- SERENO MI, DALE AM, REPPAS JB, KWONG KK, BELLIVEAU JW, BRADY TJ, ROSEN BR, AND TOOTELL RB. Borders of multiple visual areas in humans revealed by functional magnetic resonance imaging. *Science* 268: 889–893, 1995.
- SHEEDY JE. Actual measurement of fixation disparity and its use in diagnosis and treatment. *J Am Opt Assoc* 51: 1079–1084, 1980.
- SMITH AM, LEWIS BK, RUTTIMANN UE, YE FQ, SINNWELL TM, YANG Y, DUYN JH, AND FRANK JA. Investigation of low frequency drift in fMRI signal. *Neuroimage* 9: 526–533, 1999.
- SMITH AT, GREENLEE MW, SINGH KD, KRAEMER FM, AND HENNIG J. The processing of first- and second-order motion in human visual cortex assessed by functional magnetic resonance imaging (fMRI). *J Neurosci* 18: 3816–3830, 1998.
- SOMERS DC, DALE AM, SEIFFERT AE, AND TOOTELL RB. Functional MRI reveals spatially specific attentional modulation in human primary visual cortex. *Proc Natl Acad Sci USA* 96: 1663–1668, 1999.
- STEVENSON SB, CORMACK LK, AND SCHOR CM. Hyperacuity, superresolution and gap resolution in human stereopsis. *Vision Res* 29: 1597–1605, 1989.
- STILLMAN AE, HU X, AND JEROSCH-HEROLD M. Functional MRI of brain during breath holding at 4 T. *Magn Reson Imaging* 13: 893–897, 1995.
- TEO PC, SAPIRO G, AND WANDELL BA. Creating connected representations of cortical gray matter for functional MRI visualization. *IEEE Trans Med Imaging* 16: 852–863, 1997.
- TOOTELL RB, HADJIKHANI N, HALL EK, MARRETT S, VANDUFFEL W, VAUGHAN JT, AND DALE AM. The retinotopy of visual spatial attention. *Neuron* 21: 1409–1422, 1998a.
- TOOTELL RB, HADJIKHANI N, MENDOLA JD, MARRETT S, AND DALE AM. From retinotopy to recognition: fMRI in human visual cortex. *Trends Cogn Sci* 2: 174–183, 1998b.
- TOOTELL RB, MENDOLA JD, HADJIKHANI NK, LEDDEN PJ, LIU AK, REPPAS JB, SERENO MI, AND DALE AM. Functional analysis of V3A and related areas in human visual cortex. *J Neurosci* 17: 7060–7078, 1997.
- TOOTELL RB, REPPAS JB, KWONG KK, MALACH R, BORN RT, BRADY TJ, ROSEN BR, AND BELLIVEAU JW. Functional analysis of human MT and related visual cortical areas using magnetic resonance imaging. *J Neurosci* 15: 3215–3230, 1995.
- TREUE S AND MARTINEZ TRUJILLO JC. Feature-based attention influences motion processing gain in macaque visual cortex. *Nature* 399: 575–579, 1999.
- WALLACH H AND ZUCKERMAN C. The constancy of stereoscopic depth. *Am J Psychol* 76: 404–412, 1963.
- WANDELL BA, CHIAL S, AND BACKUS BT. Visualization and measurement of the cortical surface. *J Cogn Neurosci* 12: 739–752, 2000.
- WANDELL BA, POIRSON AB, NEWSOME WT, BASELER HA, BOYNTON GM, HUK A, GANDHI S, AND SHARPE LT. Color signals in human motion-selective cortex. *Neuron* 24: 901–909, 1999.
- WATANABE T, SASAKI Y, MITAUCHI S, PUTZ B, FULIMAKI N, NIELSEN M, TAKINO R, AND MIYAKAWA S. Attention-regulated activity in human primary visual cortex. *J Neurophysiol* 79: 2218–2221, 1998.
- WATSON JD, MYERS R, FRACKOWIAK RS, HAJNAL JV, WOODS RP, MAZZIOTTA JC, SHIPP S, AND ZEKI S. Area V5 of the human brain: evidence from a combined study using positron emission tomography and magnetic resonance imaging. *Cereb Cortex* 3: 79–94, 1993.
- WESTHEIMER G. Cooperative neural processes involved in stereoscopic acuity. *Exp Brain Res* 36: 585–597, 1979.
- WESTHEIMER G. Spatial interaction in the domain of disparity signals in human stereoscopic vision. *J Physiol (Lond)* 370: 619–629, 1986.
- WHEATSTONE C. Contributions to the physiology of vision: part the first. On some remarkable, and hitherto unobserved, phenomena of binocular vision. *Philos Trans R Soc Lond* 128: 371–394, 1838.
- ZEKI SM. Uniformity and diversity of structure and function in rhesus monkey prestriate visual cortex. *J Physiol (Lond)* 277: 273–290, 1978.
- ZEKI SM. Functional specialization and binocular interaction in the visual areas of rhesus monkey prestriate cortex. *Proc R Soc Lond B Biol Sci* 204: 379–397, 1979.
- ZEKI SM, WATSON JD, LUECK CJ, FRISTON KJ, KENNARD C, AND FRACKOWIAK RS. A direct demonstration of functional specialization in human visual cortex. *J Neurosci* 11: 641–649, 1991.